Roughness of Stylolites: Implications of 3D High Resolution Topography Measurements

J. Schmittbuhl
Laboratoire de Géologie, UMR CNRS 8538, Ecole Normale Supérieure, 24, rue Lhomond, F-75231 Paris Cédex 05, France

F. Renard* and J. P. Gratier
LGIT-CNRS-Observatoire, Université J. Fourier, BP 53, F-38041 Grenoble, France

R. Toussaint
Institute of Physics, University of Oslo, PB 1048, Blindern, N-0316 Oslo, Norway
(Received 3 March 2003; revised manuscript received 18 August 2004; published 1 December 2004)

Stylolites are natural pressure-dissolution surfaces in sedimentary rocks. We present 3D high resolution measurements at laboratory scales of their complex roughness. The topography is shown to be described by a self-affine scaling invariance. At large scales, the Hurst exponent is $\zeta_1 \approx 0.5$ and very different from that at small scales where $\zeta_2 \approx 1.2$. A crossover length scale at around $L_c = 1$ mm is well characterized. Measurements are consistent with a Langevin equation that describes the growth of a stylolitic interface as a competition between stabilizing long range elastic interactions at large scales or local surface tension effects at small scales and a destabilizing quenched material disorder.

DOI: 10.1103/PhysRevLett.93.238501 PACS numbers: 91.60.Dc, 62.40.+i, 68.35.Ct, 68.35.Fx

Stylolites are geological patterns that are very common in polished limestones, a material largely used to construct floors and walls of buildings and monuments. They are observed in many sedimentary rocks as thin irregular interfaces that look like printed lines on rock cuts, which is responsible for their name. They are roughly planar structures, typically perpendicular to the geological load (i.e., lithostatic pressure or tectonic maximum compressive stress) and are formed at shallow depths in the Earth's crust during deformation of sedimentary rocks. They result from a combination of stress-induced dissolution and precipitation processes [1] and exist on a very large range of scales, from micrometers to meters. Despite their abundance, stylolites are, as mentioned by Gal *et al.* [2], "among the least well-explained of all pressure-solution phenomena." First, they are complex 3D structures that are often only described from 2D cross sections since they are generally partially sealed [3]. Second, they develop in various geological contexts which lead to very different geometries. Third, they are sometimes transformed because of processes like diagenesis and metamorphism that develop after their initiation.

In this Letter we show the first 3D high resolution topography measurements of natural stylolite interfaces. We characterize the scaling invariance, namely, self-affinity, of the morphology and show the presence of a crossover length scale. We also propose a model based on a Langevin equation that emphasizes the role of the quenched disorder.

The roughness measurements have been performed on three independent stylolite interfaces included in very fine-grained limestone samples from Burgundy area, Vercors, and Jura mountains in France (Fig. 1). The samples have been collected in newly open quarries, thus preserved from late breakage and chemical erosion. The opening procedure was possible for these samples because of the accumulation of undissolved minerals like clays which formed a weak layer along the stylolite interface. The concentration of these minerals provides an estimate of the cumulative strain by dissolution the sample underwent [4]. As shown in Fig. 1, peaks along the interface are randomly distributed in space and of various sizes (up to 1 cm). Large peak magnitudes and local high slopes along the topography make the roughness measurement difficult and challenging.

We used two different profilometers to sample the stylolite roughness. First, with a mechanical profilometer [5] we extracted four profiles of 1030 points each with a horizontal step of $\Delta x = 30$ μm. The mechanical profilometer measures the surface height from the contact of a needle onto the surface (its radius is 25 μm). The vertical resolution is 3 μm over an available range of 5 cm. One of these profiles is shown in Fig. 2. We compare the me-

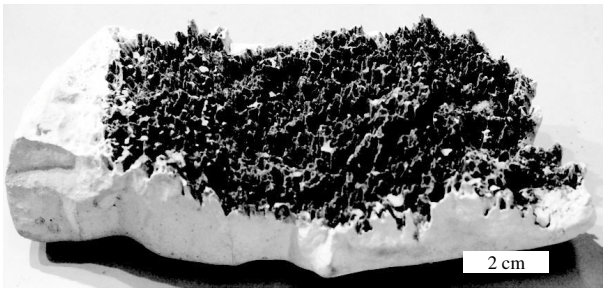

FIG. 1. Picture of a stylolite surface (S12A) in a limestone from Vercors Mountains. Magnitude of the peaks are typically of the order of 6 mm.

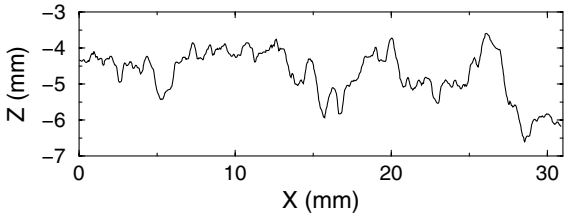

FIG. 2. A 1D profile obtained by a mechanical profilometer (1030 data points − $\Delta x = 30$ μm) along a stylolite surface.

chanical measurements to an optical profiling [6] that is based on a laser triangulation of the surface without any contact. The laser beam is 30 μm wide and horizontal steps between measurement points were $\Delta x = \Delta y = 7$ to 50 μm. The vertical resolution is 2 μm. The latter technique has a high acquisition speed since there is no vertical move, allowing on-flight measurements. However, a successful comparison with mechanical measurements is necessary to ensure that optical fluctuations are true height fluctuations and not material property fluctuations. Three independent samples have been measured at very high resolution: one side of a stylolite from Jura mountains (Sjura) with a resolution 600×600, one side of a stylolite from Burgundy area (S15) with a resolution 8200×4100, and two opposite surfaces of the same stylolite from Vercors mountains shown in Fig. 1 with a resolution 2400×1400 for S12A and 8200×4100 for S12B.

We analyzed the height distribution in terms of self-affinity [7], which states that the surface remains statistically unchanged for the transform: $\Delta x \to \lambda \Delta x$, $\Delta y \to \lambda \Delta y$, $\Delta z \to \lambda^{\zeta} \Delta z$, where λ can take any real value. The exponent ζ is the so-called Hurst exponent. A 1D average wavelet coefficient (AWC) technique [8] has been used to estimate ζ. Indeed, for a self-affine profile, the wavelet spectrum behaves as a power law with a slope $1/2 + \zeta$. AWC spectra clearly exhibit two regimes (Fig. 3). At large length scales, a power-law behavior is observed with a slope of 1, which is consistent with a Hurst exponent of $\zeta_1 = 0.5$. At small length scales, a second power-law behavior is observed with a larger slope (1.7) in agreement with a Hurst exponent $\zeta_2 = 1.2$. The crossover length scale is sharp and defines a characteristic length scale which is slightly different for the three surfaces, $L_c \approx 1$ mm. L_c is several orders of magnitude larger than the grain size and experimental cutoffs. This spectral behavior is observed for both mechanical and optical measurements.

We checked that another analysis technique, namely, the Fourier power spectrum, was providing very consistent results. Figure 4 shows averaged 1D spectra of profiles extracted from the surface Sjura. A self-affine property of the profiles leads to a power-law behavior of the power spectrum as $P(k) \propto k^{-1-2\zeta}$ [7]. Moreover, average spectra of profiles taken along perpendicular directions provide very consistent results (Fig. 4). Isotropy of scaling invariance is confirmed by the circular symmetry of the 2D power spectrum of the surface.

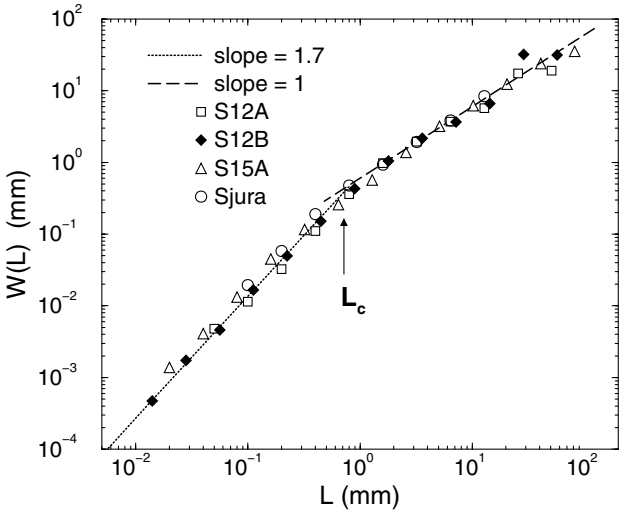

FIG. 3. Averaged wavelet spectra of topographic profiles extracted from four optical maps of stylolite surfaces. Spectra have been normalized to superimpose for large L on the spectrum of S12A.

The second part of the Letter is devoted to a modeling of the stylolite roughening which aims at understanding the origin of the self-affine behaviors and of the characteristic length L_c. The stylolite interface is assumed to be initiated along a boundary between geological beds. More precisely it is approximated as the boundary of a quasiflat and very elongated fluid pore where the trapped fluid is

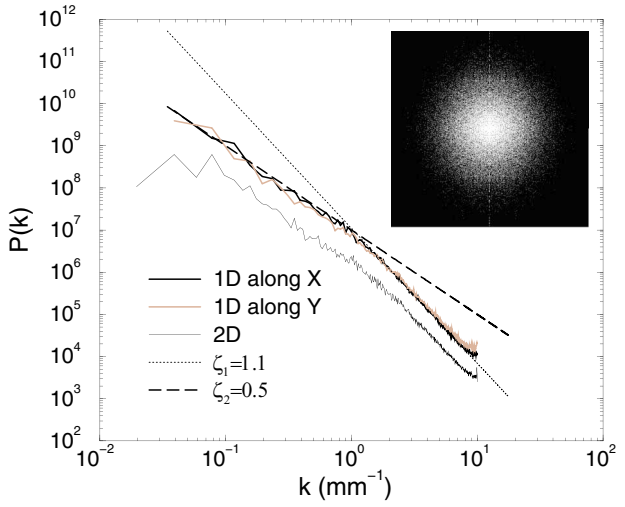

FIG. 4 (color online). Fourier power spectra of 1D topographic profiles oriented along two perpendicular directions (X and Y) and of the full 2D surface. The latter was radially integrated to be compared to the 1D power spectra. Inset: A gray map of the 2D power spectrum. A mirroring technique has been used to reduce nonperiodic edge effects.

assumed to be at lithostatic pressure and the solid, where this pore is embedded, at an average stress $\boldsymbol{\sigma}^0 = \sigma^0_{zz}\hat{z}\,\hat{z} + \sigma^0_{xx}(\hat{x}\,\hat{x} + \hat{y}\,\hat{y})$, where $\hat{z}$ refers to the direction normal to average stylolite direction and $\hat{x}$ and $\hat{y}$ refer to directions along the average stylolite direction. Since stylolites are on average normal to the largest principal stress direction, $\sigma_s = |\sigma^0_{zz}| - |\sigma^0_{xx}| > 0$.

Possible solid contacts with the mirror surface on the other side of the fluid film are neglected, considering that such contact points concentrate dissolution and disappear. Accordingly, we assume that the stylolite morphology is to first order dominated by a dissolution process between a fluid film and a single elastic solid.

Assuming a free surface profile $z(x, t)$, the normal $\hat{n}$ to the interface pointing toward the solid is, in the limit of small relief, $\hat{n} = \hat{z} - (\partial_x z)\hat{x}$, where plane strain holds. The stress state in the solid is expressed as $\boldsymbol{\sigma} = \boldsymbol{\sigma}^0 + \boldsymbol{\sigma}^1$, where mechanical equilibrium between solid and fluid requires that $\boldsymbol{\sigma}^1 \cdot (-\hat{n}) = -\sigma_s(\partial_x z)\hat{x}$. This stress state results from a surface distribution of tangential force $-\sigma_s(\partial_x z)\hat{x}$ applied on the quasiplanar boundary of the solid by the fluid, so that using Green's elastostatic function [9] and integrating along the y direction, at the surface, $\sigma^1_{xz} = \sigma^1_{zx} = \sigma_s(\partial_x z)$ and $\sigma^1_{xx} = \sigma^1_{yy} = \sigma_s(2\nu/\pi) \times \int dy(\partial_y z(y))/(x - y)$, all other components being null.

For small reliefs ($||\sigma_1||/||\sigma_0|| \ll 1$) and to the leading order, the elastic free energy $u_e = [(1 + \nu)\sigma_{ij}\sigma_{ij} - \nu\sigma_{kk}\sigma_{ll}]/4E$ can be approximated as $u_e = u^0_e + u^1_e$ where, from the above, $u^0_e = \alpha p_0^2/E$, and

$$u^1_e = -\beta(p_0\sigma_s/E)\int dy(\partial_y z)/(x - y) \qquad (1)$$

with an average solid pressure $p_0 = -(2\sigma^0_{xx} + \sigma^0_{zz})/3$, and two dimensionless positive constants $\alpha = [9(1 - 2\nu) + 2(1 + \nu)\sigma_s^2/p_0^2]/12$ and $\beta = \nu(1 - 2\nu)/\pi$, where E is an effective Young's modulus, and ν the Poisson coefficient. u^0_e is the average elastic energy from the global tectonic loading and u^1_e is its local perturbation that results from the interface topography.

The chemical potential difference at the solid-fluid interface that potentially destabilizes the interface can be written as [10] $\Delta\mu = \Omega(u_e + \gamma\kappa)$ where u_e is the elastic energy per unit volume in the solid, γ is the surface energy, κ is the curvature, and Ω is a molar volume. Gravity effects are supposed to be negligible. We have also assumed that the matrix of the solid, i.e., an assembly of initial sedimentary particles, is sufficiently porous during stylolite initiation to have a bulk diffusion within the material. This assumption is supported by rock thin section observations under an optical microscope [11]. If a bulk diffusion holds in the fluid surrounding the stylolite, the evolution of the interface is directly related to the chemical potential difference: $v_n = m\Delta\mu$ where v_n is the normal dissolution velocity and m is the mobility [10]. We also neglected the chemical potential evolution within the film since we aim only at describing the initiation of the process under drained conditions.

This homogeneous description thus predicts, for small reliefs, $\partial_t z = v_0 + m\Omega(u^1_e + \gamma\partial_{xx} z)$, with $v_0 = m\Omega u^0_e$. Surface tension is a stabilizing term, but it is important to note that the elastic interaction term, u^1_e, is also stabilizing in the present context. For the present situation, stylolites are perpendicular to the maximum principal stress, and will subsequently be assumed horizontal: $\sigma_s > 0$. Considering an elementary departure from a flat interface, such as a fluid intrusion in the solid, i.e., a bump with a maximum in x, such as $\partial_y z > 0$ for $y < x$, and $\partial_y z < 0$ for $y > x$, u^1_e is negative in x and reduces the dissolution speed in the bump at x. Accordingly, since the problem is linear, elastic interactions are stabilizing for any corrugations of the interface. For vertical stylolites, the picture is opposite ($\sigma_s < 0$) and elastic interactions are destabilizing leading to the growth of horizontal fingers.

The homogeneous picture predicts the propagation of a planar dissolution interface driven by the average elastic energy u^0_e, with an average speed estimated as $v_0 \approx 8 \times 10^{-6}$ m/yr where we used $m = k\Omega/(RT)$, with a dissolution rate $k \approx 10^{-4}$ mol/m^2/s, $\Omega \approx 4 \times 10^{-5}$ m^3/mol for calcite, R is the universal gas constant, $T \approx 300$ K, $\alpha \approx 0.5$, $E \approx 8 \times 10^{10}$ Pa for limestones, a characteristic stress estimated as $p_0 \approx 25$ MPa, corresponding to a rock at 1 km depth.

To understand the dynamic roughening of stylolites, it is essential to capture the effect of heterogeneities of relevant material properties in the solid, namely ν, E, m, and γ. We assume the relative variation ($\delta E/E$ and others) of these properties to be small, and to correspond to independent random variables associated with each constitutive grain of the rock, which are typically $\ell = 10\ \mu$m sized. At early stages of the process where $\partial_x z \ll 1$, we define the dimensionless surface position with respect to the average plane $z' = (z - v_0 t)/\ell$ and the dimensionless space and time variables $x' = x/\ell$ and $t' = t/\tau$ where $\tau = \ell^2/(\gamma\Omega m)$ to obtain, to the leading order in relative fluctuations and typical slopes, for the roughening interface speed

$$\partial_{t'} z'(x', t') = \partial_{x'x'} z' - \frac{\ell}{L^*}\int dy' \frac{\partial_{y'} z'}{x' - y'} + \eta(x', z'(x')), \qquad (2)$$

where $L^* = \gamma E/(\beta p_0 \sigma_s)$ and $\eta = [\alpha\ell p_0/(\beta L^* \sigma_s)] \times [(\delta E/E) + (\delta m/m) - (\delta\alpha/\alpha)]$. In this Langevin equation with quenched noise, the destabilizing random term is balanced by the restoring surface tension term at scales below L^*, and by the restoring elastic interactions at scales above L^*. We propose that this critical scale L^* corresponds to the measured crossover length L_c. For typical limestones, $\gamma = 0.27$ J/m^2 for a water-calcite

surface and $\nu \approx 0.25$, so that $\beta \approx 0.04$ and $L^* \approx 0.9$ mm, consistently with the above measured. The other characteristic quantities of interest are $\tau \approx 0.2$ yr, and the characteristic amplitude of the dimensionless noise η is $\rho \approx \alpha \ell p_0/(\beta \lambda^* \sigma_s) \approx 0.2$.

For the Laplacian regime ($L \ll L^*$) and the mechanical regime ($L \gg L^*$), only one of the two restoring terms in Eq. (2) dominates, and these two independent regimes have already been studied. Indeed, the Laplacian regime is nothing other than the Edwards Wilkinson (EW) problem [12] in a quenched noise. In this case the interface is self-affine with an exponent $\zeta_2 \approx 1.2$ [13]. In the mechanical regime, Eq. (2) is analogous to the quasistatic propagation of an elastic line or a mode I fracture front in a disordered material, and the Hurst exponent is $\zeta_1 \approx 0.4$ for a kernel similar to Eq. (1) [14].

The roughening amplitude can be obtained by considering the EW equation with a quenched noise: the characteristic width of the surface measured at scale L, i.e., the saturation width, scales as $w(L)/\ell \approx \rho(L/\ell)^{\zeta_2}$. The saturation time for this width to be achieved from a flat interface defines the characteristic time for the roughness evolution $\tau_s(L)$. Indeed, the dissolution process goes on, with an average speed v_0, as long as $u_e^0 > 0$, and the surface profile fluctuates around the average progressing plane with a correlation time τ_s and a characteristic amplitude $w(L)$. τ_s is such that $\tau_s/\tau \approx (L/\ell)^{\zeta_2/\delta}$, with a dynamic exponent $\delta \approx 0.8$ [13]. With $L \approx 1$ mm, $\ell \approx 10\ \mu$m, and $\zeta_2 \approx 1.2$, this scaling law predicts, up to a constant of order unity, the saturation width at crossover scale $w(L^*) \approx 0.5$ mm and the time to saturation as $\tau_s \approx 200$ yr. This length scale corresponds to the measured one (Fig. 2). The short saturation time implies that observed stylolites have achieved their saturation width over geological time scales. That the width amplitude is also correctly predicted in the mechanical regime could be checked directly, but is granted by the fact that it is correctly predicted in the Laplacian regime, as well as the crossover scale, which determines entirely the prefactor of the scaling law $w(L)$ in the $L > L^*$ regime. In principle, determining L^* and $w(L^*)$ could give two independent constraints on both p_0 and σ_s, which could allow one to determine both the pressure and the differential stress prevailing during the formation of a particular stylolite. However, given the amount of approximations in the involved constants, the only way to test this effect on the crossover wavelength would be to measure stylolites formed in various geological conditions and study the effect of depth and orientation to the main stress.

In conclusion, we presented a quantitative description of stylolite interfaces. The experimental measurements are 3D high resolution descriptions of the topography of natural stylolites. We show that the surfaces are self-affine but with two regimes. At small scales, the Hurst exponent is unexpectedly high, $\zeta_2 = 1.2$, and consistent with a Laplacian regime. At large scales, the stylolites morphology is controlled by long range elastic stress redistributions. In this case the roughening is important with a low Hurst exponent $\zeta_1 = 0.5$. The two regimes are separated by a crossover characteristic length L_c, also predicted by a model based on the description of a stress-induced dissolution, where restoring surface tension effects and elastic interactions compete with a quenched noise. It is important for geological implications to note that L_c is very sensitive to the average stress p_0. Indeed, a measurement of L_c from roughness profiling could provide an estimate of the stress magnitude during the stylolite growth, that is, in the past. Accordingly, stylolites could be considered as stress fossils.

We acknowledge D. Rothman, J. Rice, A. Lobkovsky, B. Evans, Y. Bernabé, B. Goffé, H. Perfettini, P. Meakin, and E. Merino for fruitful discussions.

*Also at Physics of Geological Processes, University of Oslo, Norway.

[1] W. C. Park and E. H. Schot, J. Sediment. Petrol. **38**, 175 (1968).
[2] D. Gal, A. Nur, and E. Aharonov, Geophys. Res. Lett. **25**, 1237 (1998).
[3] Z. Karcz and C. H. Scholz, J. Struct. Geol. **25**, 1301 (2003).
[4] F. Renard *et al.*, J. Geophys. Res. **109**, B03209 (2004).
[5] J. Lopez and J. Schmittbuhl, Phys. Rev. E **57**, 6405 (1998).
[6] Y. Méheust, Ph.D. thesis, University Paris 11, 2002.
[7] A. Barabási and H. Stanley, in *Fractal Concepts in Surface Growth*, edited by A. Barabási and H. Stanley (Cambridge University Press, Cambridge, 1995).
[8] I. Simonsen, A. Hansen, and O. M. Nes, Phys. Rev. E **58**, 2779 (1998).
[9] L. D. Landau and E. M. Lifchitz, *Theory of Elasticity* (Butterworth-Heinemann, London, 1986), 3rd ed.
[10] K. Kassner *et al.*, Phys. Rev. E **63**, 036117 (2001).
[11] E. Carrio-Schaffhauser and S. Raynaud, J. Struct. Geol. **14**, 973 (1992).
[12] S. E. Edwards and D. R. Wilkinson, Proc. R. Soc. London A **381**, 17 (1982).
[13] S. Roux and A. Hansen, J. Phys. I (France) **4**, 515 (1994).
[14] J. Schmittbuhl, S. Roux, J. P. Vilotte, and K. Måløy, Phys. Rev. Lett. **74**, 1787 (1995); S. Ramanathan and D. S. Fisher, Phys. Rev. B **58**, 6026 (1998); A. Tanguy, M. Gounelle, and S. Roux, Phys. Rev. E **58**, 1577 (1998); A. Rosso and W. Krauth, Phys. Rev. E **65**, 025101(R) (2002).